Measurements of Photon Correlations in a Laser Beam near Threshold with Time-to-Amplitude Converter Techniques*

F. DAVIDSON†
Department of Physics and Astronomy, The University of Rochester, Rochester, New York 14627
(Received 28 October 1968; revised manuscript received 11 February (1969)

A procedure for the measurement of intensity correlations of the type $\langle:\hat{I}(\mathbf{x},t)\hat{I}(\mathbf{x},t+\tau):\rangle$ and $\langle:\hat{I}(\mathbf{x},t)\times\hat{I}(\mathbf{x},t+\tau_1)\hat{I}(\mathbf{x},t+\tau_2):\rangle$ with the use of a time-to-amplitude converter is developed. The procedure is used to measure second- and third-order intensity fluctuation correlation functions of the optical field produced by a gas laser operated at various levels near its threshold of oscillation. The results are shown to be in agreement with the predictions of laser theories.

I. INTRODUCTION

THE correlation functions of a stationary optical field contain information about the nature of the radiation field, and, indirectly, about the nature of the source.[1–4] The most elementary correlation function that can be measured is one in which the optical field strength is sampled at two space-time points and the mean value of the product is formed. This type of correlation function is referred to as a second-order correlation function and is usually measured with the use of an interferometer.

Higher-order correlation functions of optical fields are also of interest and are experimentally measured with the use of photoelectric detectors. The second-order intensity correlation function, or fourth-order field amplitude correlation function, is defined[5] as the trace of the product of a diagonal density operator and normally ordered operators corresponding to the negative- and positive-frequency components of the operator that represents the second quantized description of the electromagnetic field at two space-time points. An arbitrary nth-order intensity correlation function, or $2n$th field amplitude correlation function, is similarly defined as the trace of the product of a diagonal density operator with appropriate normally ordered operators representing the positive- and negative-frequency components of the electromagnetic field at n space-time points.

Glauber[6,7] has shown, with the aid of a heuristic argument, that the joint probability of two photodetectors, one located at $\mathbf{x}_1$, the other at $\mathbf{x}_2$, absorbing one photon at point $\mathbf{x}_1$ at time t_1 within Δt_1, and another photon at point $\mathbf{x}_2$ at time $t_1+\tau$ within $\Delta\tau$ is proportional to the second-order intensity correlation function of the optical field incident on the detectors. This second-order intensity correlation function is denoted by $\langle:\hat{I}(\mathbf{x}_1,t_1)\hat{I}(\mathbf{x}_2,t_1+\tau):\rangle$, where the symbol :: means the operators that represent the field intensity appear in normal order, and the angular brackets denote that a trace of the product of the density operator and the normally ordered operators is to be taken. Later work[8–10] indicated that the results of Glauber's argument were correct and that the twofold joint probability of two photodetectors absorbing a photon at the space-time points $\mathbf{x}_1$, t_1, $\mathbf{x}_2$, $t_1+\tau$ within time intervals Δt_1 and $\Delta\tau$ was given by $\alpha_1 c S_1 \Delta t_1 \alpha_2 c S_2 \Delta\tau\langle:\hat{I}(\mathbf{x}_1,t_1)\hat{I}(\mathbf{x}_2,\ t_1+\tau):\rangle$, where α_1 and α_2 are the dimensionless quantum efficiencies of the photodetectors, and S_1 and S_2 are their surface areas.

Second-order intensity correlation functions of the type $\langle:\hat{I}(\mathbf{x}_1,t_1)\hat{I}(\mathbf{x}_2,\ t_1+\tau):\rangle$ have been measured with the use of analog photomultiplier signal-correlation apparatus, as in the Hanbury Brown-Twiss experiments,[11] and also with the use of a coincidence counter,[12] that measured the twofold joint probability of photon absorption at two different space-time points. Analog signal-correlation techniques do not directly yield the correlation function $\langle:\hat{I}(\mathbf{x}_1,t_1)\hat{I}(\mathbf{x}_2,\ t_1+\tau):\rangle$ but give a related quantity[13] and are best suited to situations where the optical field is strong enough to produce high photomultiplier counting rates. The use of a coincidence counter requires the use of calibrated lengths of delay cable to study $\langle:\hat{I}(\mathbf{x}_1,t_1)\hat{I}(\mathbf{x}_2,\ t_1+\tau):\rangle$ as a function of τ, and requires a separate measurement for each value of τ considered.

Measurements of the probability $P(n,T)$ of one photodetector registering n counts in a counting time T have also been made to obtain information about

* Work supported by the Air Force Cambridge Research Laboratories and by the U. S. Air Force Office of Scientific Research, Office of Aerospace.
† Present address: Cullen College of Engineering, University of Houston, Houston, Tex.
[1] M. Born and E. Wolf, *Principles of Optics* (The Macmillan Co., New York, 1964), 2nd rev. ed., Chap. X.
[2] L. Mandel and E. Wolf, Rev. Mod. Phys. **37**, 231 (1965).
[3] R. J. Glauber, in *Quantum Optics and Electronics*, edited by C. DeWitt, A. Blandin, and C. Cohen-Tannoudji (Gordon and Breach, Science Publishers, Inc., New York, 1965), p. 65.
[4] L. Mandel, in *Proceedings of the Symposium on Modern Optics* (Polytechnic Press of Polytechnic Institute of Brooklyn, New York, 1967), Vol. XVII, p. 143.
[5] R. J. Glauber, Phys. Rev. **130**, 2529 (1963).
[6] R. J. Glauber, Phys. Rev. **131**, 2766 (1963).
[7] R. J. Glauber, Phys. Rev. Letters **10**, 84 (1963).
[8] E. C. G. Sudarshan, Phys. Rev. Letters **10**, 277 (1963).
[9] P. L. Kelley and W. H. Kleiner, Phys. Rev. **136**, A316 (1964).
[10] L. Mandel, E. C. G. Sudarshan, and E. Wolf, Proc. Phys. Soc. (London) **84**, 435 (1964).
[11] R. Hanbury Brown and R. Q. Twiss, Nature **177**, 27 (1956).
[12] R. Hanbury Brown, A. G. Little, and R. Q. Twiss, Nature **180**, 324 (1957).
[13] R. Hanbury Brown and R. Q. Twiss, Proc. Roy. Soc. (London) **A243**, 291 (1958).

second-order intensity correlation functions.[14] The fluctuation in the square of the number of counts observed in a counting time T, $\langle(\Delta n_T)^2\rangle$ is related to the correlation properties of the optical field incident on the photodetector.[15]

Analysis of the frequency spectrum of the fluctuations in the output current of a photomultiplier has also been used as a means of experimentally measuring second-order intensity correlation functions.[16,17] If the optical field is stationary, the Fourier transform of the square of the frequency spectrum of the photomultiplier output current fluctuations can be related to the second-order intensity fluctuation correlation function.[4,18]

It was the purpose of this investigation to develop a method for the measurement of second- and third-order intensity correlation functions, and to apply it to the study of a gas laser beam. It was found that the desired measurements could be made with the use of a time-to-amplitude converter (TAC), and that this method would have the following advantages over the other possible methods: (1) While the TAC output data are not as directly related to the desired intensity correlation functions as the data obtained from a coincidence counter, the TAC accumulates data at a much higher rate and does not require separate measurements for each τ value considered; (2) since the TAC processes individual photoelectron pulses, measurements can be made on very weak optical fields. Both analog signal correlation measurements and frequency spectrum measurements on photomultiplier current fluctuations require high photomultiplier counting rates and work well only on optical fields intense enough to produce high photodetector counting rates; (3) while detailed information about intensity correlation functions is obtainable from $P(n,T)$ measurements, it was found that less data and computation were necessary to determine the behavior of second- and third-order intensity correlation functions with the use of TAC. Some preliminary results of measurements made with TAC techniques of intensity correlation functions of a gas laser beam have already been reported.[19,20]

Section II gives a brief outline of the method used to make measurements of second- and third-order intensity correlation functions with the use of a TAC. Section III describes the experimental apparatus used to measure these correlation functions of a gas laser operating near its threshold of oscillation. Section IV compares the experimental results with the theoretically expected behavior of a gas laser operated near threshold.

II. THEORY OF CORRELATION MEASUREMENTS WITH TAC

The correlation function $\langle:\hat{I}(\mathbf{x}_1,t_1)\hat{I}(\mathbf{x}_2,t_1+\tau):\rangle$ can be found from a measurement of the joint probability of photoelectric detection of two photons, one at space-time point $\mathbf{x}_1,t_1$ within time Δt_1 and the other at space-time point $\mathbf{x}_2$, $t_1+\tau$ within time $\Delta\tau$. A TAC is a device which measures a quantity closely related to this joint probability, $P_2(\mathbf{x}_1,t_1,\mathbf{x}_2,t_1+\tau)\Delta t_1\Delta\tau$. It operates as follows: Photoelectron pulses from one photodetector are fed to the "start" channel of the TAC, and photoelectron pulses from a second photodetector are fed to the "stop" channel of the TAC. Once a start pulse has been received, the unit begins charging a conversion capacitor linearly with time. With the next stop pulse the charging process stops. The voltage accumulated on the conversion capacitor is transformed into an output pulse whose height is linearly proportional to the time interval between the start and stop pulses. The output pulse is then fed to a pulse-height analyzer for storage. Once the TAC starts, all other start pulses are ignored until the unit has either made a conversion or has fully charged the conversion capacitor and reset it to zero volts. No stop pulses are accepted until a start pulse has initiated the conversion process. Once a stop pulse has been accepted and a conversion made, all other stop pulses are ignored until the unit has been completely reset and a valid start pulse has again initiated the conversion process. If no stop pulse arrives to stop the charging process before the conversion capacitor is fully charged, the unit produces no output pulse, and resets as soon as the capacitor is fully discharged.

A detailed mathematical analysis of the operation of the TAC has already been presented.[21] The results of that analysis are as follows. The rate $R(\tau)$ at which TAC conversions corresponding to start and stop pulses spaced τ seconds apart are stored in one channel of width $\Delta\tau$ of a pulse-height analyzer is given by a modified twofold joint probability, $\tilde{P}_2(\mathbf{x}_1,t_1,\mathbf{x}_2,t_1+\tau;$ no stops in $t_1-T_L<t_j<t_1+\tau;$ no starts in $t_1-T_W<t_k<t_1)\Delta\tau$. T_W is the conversion range in seconds of the TAC, and T_L is the delay introduced in the TAC stop channel, so that conversions corresponding to the simultaneous arrival of start and stop pulses are not recorded in channel 0 of the pulse-height analyzer. Some TAC conversions will not be recorded because of dead time losses of the TAC. With the inclusion of dead time losses and a quantitative expression for the modified twofold

[14] See, e.g., J. A. Armstrong and A. W. Smith, Phys. Rev. Letters **16**, 1169 (1965).

[15] L. Mandel, Proc. Phys. Soc. (London) **72**, 1037 (1958).

[16] P. J. Bolwijn, C. T. J. Alkemade, and G. A. Boschloo, Phys. Letters **4**, 59 (1966).

[17] C. Freed and H. Haus, Phys. Rev. **141**, 287 (1966).

[18] A. M. Yaglom, *An Introduction to the Theory of Stationary Random Functions* (Prentice-Hall, Englewood Cliffs, N. J., 1962), Chap. II.

[19] F. Davidson and L. Mandel, Phys. Letters **25A**, 700 (1967).

[20] F. Davidson and L. Mandel, Phys. Letters **27A**, 579 (1968).

[21] F. Davidson and L. Mandel, J. Appl. Phys. **39**, 62 (1968).

joint probability, $R(\tau)$ can be expressed as

$$R(\tau)=\alpha_1\alpha_2c^2S_1S_2\Delta\tau\Big\langle:\hat{I}(\mathbf{x}_1,t_1)\hat{I}(\mathbf{x}_2,t_1+\tau)\times\exp\Big(-\alpha_2cS_2\int_{t_1-T_L}^{t_1+\tau}\hat{I}(\mathbf{x}_2,t')dt'\Big)\times\exp\Big(-\alpha_1cS_1\int_{t_1-T_W}^{t_1}\hat{I}(\mathbf{x}_1,t')dt'\Big):\Big\rangle\times\exp[-(\text{TAC conversion rate})\times(\text{dead time})]. \quad (1)$$

If the stationary optical field incident on the photodetectors contains no correlated intensity fluctuations, Eq. (1) reduces to

$$R(\tau)=R_1R_2\Delta\tau\exp[-R_2(T_L+\tau)-R_1T_W]\times\exp[-(\text{TAC conversion rate})\times(\text{dead time})], \quad (2)$$

where R_1 and R_2 are the photodetector average counting rates, given by $\alpha_1cS_1\langle:\hat{I}(\mathbf{x}_1):\rangle$ and $\alpha_2cS_2\langle:\hat{I}(\mathbf{x}_2):\rangle$, respectively. If the average counting rates are kept sufficiently low, and beam splitters are used so that both photodetectors view the same point of the optical field, Eq. (1) can be expanded to yield the following integral equation for $\lambda(\tau)$, a second-order intensity fluctuation correlation function:

$$\lambda(\tau)=\frac{1}{\theta_1\theta_2}\xi(\tau)+R_1\int_{\tau}^{\tau+T_W}\lambda(\tau')d\tau'+R_2\frac{\theta_2}{\theta_1}\int_0^{\tau+T_L}\lambda(\tau')d\tau'+R_1\frac{\theta_1}{\theta_2}\int_0^{T_W}\lambda(\tau')d\tau'+R_2\int_{-T_L}^{\tau}\lambda(\tau')d\tau', \quad (3a)$$

where θ_i is the phototube dark-current correction factor and is calculated by subtracting from the photodetector average counting rate the photodetector average background counting rate and then dividing by the photodetector average counting rate. $\lambda(\tau)$ is defined as

$$\lambda(\tau)=\frac{\langle:\Delta\hat{I}(\mathbf{x},t_1)\Delta\hat{I}(\mathbf{x},t_1+\tau):\rangle}{\langle:\hat{I}(\mathbf{x}):\rangle\langle:\hat{I}(\mathbf{x}):\rangle} \quad (3b)$$

and $\xi(\tau)$ is the normalized excess rate at which the conversions are made for photons spaced τ sec apart;

$$\xi(\tau)=\frac{R(\tau)-R_1R_2\Delta\tau\exp[-R_2(T_L+\tau)-R_1T_W]\exp[-(\text{TAC conversion rate})\times(\text{dead time})]}{R_1R_2\Delta\tau\exp[-R_2(T_L+\tau)-R_1T_W]\exp[-(\text{TAC conversion rate})\times(\text{dead time})]}. \quad (3c)$$

Equation (3a) can be solved by iteration, with the zeroth-order solution for $\lambda(\tau)$ taken to be the measured quantity $\xi(\tau)$. The convergence of the equation will be illustrated in Sec. IV. Equation (3a) is accurate only if R_1T_W and R_2T_L are kept very small compared to unity.

Third-order intensity correlation functions can also be measured with TAC, by starting the TAC with the output of a coincidence unit fed by two photodetectors. The rate at which TAC conversions are made, $R(\tau_1,\tau_2)$, is given by a modified threefold joint probability that a photon is absorbed at the space-time points $\mathbf{x}_1,t_1$ within a time Δt_1, $\mathbf{x}_2$, $t_1+\tau_1$ within a time $\Delta\tau_1$, and $\mathbf{x}_3$, $t_1+\tau_2$ within a time $\Delta\tau_2$;

$$R(\tau_1,\tau_2)=\int_{\tau_1-T}^{\tau_1+T}\tilde{P}_3(\mathbf{x}_1,t_1,\mathbf{x}_2,t_1+\tau_1',\mathbf{x}_3,t_1+\tau_2;\text{ no stops in }t_1-T_L<t_j<t_1+\tau_2;\text{ no coincidences in }t_1-T_W<t_k<t_1)d\tau_1'\Delta\tau_2.$$

T is the width of the pulses fed to the coincidence unit and τ_1 is a delay created with a cable inserted between one photodetector and the coincidence logic unit. With the substitution of a quantitative expression for $\tilde{P}_3$ and the approximation that $2T$ is much less than the time over which second-order intensity correlations persist, the expression for $R(\tau_1,\tau_2)$, the rate at which conversions are stored in one channel of width $\Delta\tau_2$ of the pulse-height analyzer, becomes

$$R(\tau_1,\tau_2)=\alpha_1\alpha_2\alpha_3c^3S_1S_2S_32T\Delta\tau_2\Big\langle:\hat{I}(\mathbf{x}_1,t_1)\hat{I}(\mathbf{x}_2,t_1+\tau_1)\hat{I}(\mathbf{x}_3,t_1+\tau_2)\exp\Big(-\alpha_3cS_3\int_{t_1-T_L}^{t_1+\tau_2}\hat{I}(\mathbf{x}_3,t_1')dt_1'\Big)\times\exp\Big(-\alpha_1\alpha_2c^2S_1S_22T\int_{t_1-T_W}^{t_1}\hat{I}(\mathbf{x}_1,t_1')\hat{I}(\mathbf{x}_2,t_1'+\tau_1)dt_1':\Big\rangle\exp[-(\text{TAC conversion rate})\times(\text{dead time})]. \quad (4)$$

If the quantities R_3T_L and $R_1R_22TT_W$ are kept small compared to unity, and if beam splitters are used so that all three photodetectors view the same point of the optical field, then Eq. (4) can be expanded to yield the following

integral equation for the third-order intensity fluctuation correlation function $\lambda(\tau_1, \tau_2)$:

$$\lambda(\tau_1,\tau_2)=\frac{1}{\theta_1\theta_2\theta_3}\xi(\tau_1,\tau_2)-\frac{1}{\theta_3}\lambda(\tau_1)-\frac{1}{\theta_1}\lambda(-\tau_1+\tau_2)-\frac{1}{\theta_2}\lambda(\tau_2)+\frac{R_3}{\theta_1}\int_{-T_L}^{\tau_2}\lambda(-\tau_1+\tau')d\tau'+\frac{R_3}{\theta_2}\int_{-T_L}^{\tau_2}\lambda(\tau')d\tau'$$

$$+R_3\frac{\theta_3}{\theta_2}\int_{-T_L}^{\tau_2}\lambda(\tau_2,\tau')d\tau'+R_3\int_{-T_L}^{\tau_2}\lambda(\tau_1,\tau')d\tau'+\frac{R_3\theta_3}{\theta_1\theta_2}\int_{-T_L}^{\tau_2}\lambda(-\tau_2+\tau')d\tau'+\frac{R_3\theta_3}{\theta_1}\int_{-T_L}^{\tau_2}\lambda(-\tau_1+\tau_2,\,-\tau_1+\tau')d\tau', \quad (5a)$$

where

$$\lambda(\tau_1,\tau_2)=\frac{\langle:\Delta\hat{I}(\mathbf{x},t_1)\Delta\hat{I}(\mathbf{x},\,t_1+\tau_1)\Delta\hat{I}(\mathbf{x},\,t_1+\tau_2):\rangle}{\langle:\hat{I}(\mathbf{x}):\rangle^3}. \quad (5b)$$

$\xi(\tau_1,\tau_2)$ is the normalized excess rate at which conversions are made that correspond to detection of photons at the space-time points;

$$\xi(\tau_1,\tau_2)=\frac{R(\tau_1,\tau_2)-R_1R_2R_3 2T\Delta\tau_2\exp[-R_1R_2 2TT_W-R_3(T_L+\tau_2)-(\text{TAC conversion rate})\times(\text{dead time})]}{R_1R_2R_3 2T\Delta\tau_2\exp[-R_1R_2 2TT_W-R_3(T_L+\tau_2)-(\text{TAC conversion rate})\times(\text{dead time})]}. \quad (5c)$$

A rigorous solution of the integral Eq. (5a) would require detailed knowledge of the normalized measured excess $\xi(\tau_1,\tau_2)$ as a function of both τ_1 and τ_2. Detailed information about $\xi(\tau_1,\tau_2)$ as a function of τ_2 was available from the data in the pulse-height analyzer that stored the TAC conversions. Information about $\xi(\tau_1,\tau_2)$ as a function of τ_1 could only be obtained with the use of calibrated lengths of delay cable inserted between one photodetector and the coincidence logic unit. Since equally detailed information about the τ_1 and τ_2 dependence of $\xi(\tau_1,\tau_2)$ was unavailable, τ_1 was treated as a constant in Eq. (5a), which then was reduced to an integral equation containing only one variable.

$$\lambda(\tau_1,\tau_2)=\frac{1}{\theta_1\theta_2\theta_3}\xi(\tau_1,\tau_2)-\frac{1}{\theta_3}\lambda(\tau_1)-\frac{1}{\theta_1}\lambda(-\tau_1+\tau_2)-\frac{1}{\theta_2}\lambda(\tau_2)+\frac{R_3}{\theta_1}\int_{-T_L}^{\tau_2}\lambda(-\tau_1+\tau')d\tau'+\frac{R_3}{\theta_2}\int_{-T_L}^{\tau_2}\lambda(\tau')d\tau'$$

$$+R_3\frac{\theta_3}{\theta_2}\int_{-T_L}^{\tau_1}\lambda(\tau_1,\tau')d\tau'+R_3\int_{-T_L}^{\tau_2}\lambda(\tau_1,\tau')d\tau'+\frac{R_3\theta_3}{\theta_1\theta_2}\int_{-T_L}^{\tau_2}\lambda(-\tau_2+\tau')d\tau'+R_3\frac{\theta_3}{\theta_1}\int_{-T_L}^{0}\lambda(-\tau_1,\,-\tau_1+\tau')d\tau'. \quad (6)$$

Equation (6) was solved by iteration. The zeroth-order solution was computed from the normalized measured excess and the terms involving the known second-order intensity fluctuation correlation functions $\lambda(\tau)$. The convergence of the iteration process will be discussed in Sec. IV.

III. EXPERIMENTAL APPARATUS AND PROCEDURES

Figure 1 is a block diagram of the apparatus used to make measurements of second-order intensity correlation functions of the optical field produced by a laser operated near its threshold of oscillation. The laser used was a Spectra Physics 119, single-mode He-Ne laser that had one mirror of the optical resonant cavity mounted on a piezoelectric cylinder. The plasma tube was slightly misaligned in the optical cavity so that only certain positions of the movable mirror would provide enough cavity gain for oscillation to occur.[22] The laser was operated at an arbitrary intensity in the threshold region with the use of an amplitude stabilization feedback control circuit that sensed the laser's average intensity and applied a control voltage across the piezoelectric cylinder that determined the position of the mirror attached to it. The control circuit consisted of an integrator with a 0.1-sec time constant, a dc bias and a pentode dc amplifier. The laser's average intensity was varied by changes in the dc bias in the input to the

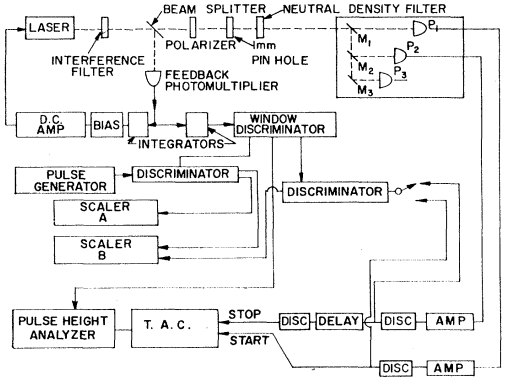

FIG. 1. Block diagram of the apparatus used to measure second-order intensity correlation functions.

[22] H. Gamo, R. Grace, and T. Walters, in Proceedings of the Second Rochester Conference on Coherence and Quantum Optics, 1966, p. 183 (unpublished).

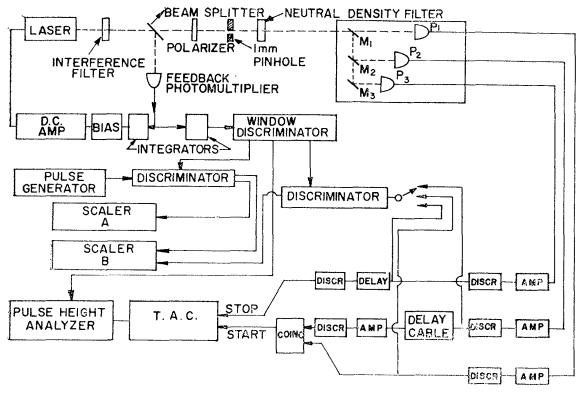

FIG. 2. Block diagram of the apparatus used to measure third-order intensity correlation functions.

dc amplifier. The interference filter, polarizer, and 1-mm pinhole isolated the 6328-Å emission line and exposed the photodetectors P1, P2, and P3 to spatially coherent light of one degree of polarization.

Individual photoelectron pulses from the photomultiplier tubes (type RCA 4459) P1 and P2 were amplified, shaped by fast discriminators, and fed to the start and stop inputs of the TAC. The TAC output pulses were stored in the channels of a 100-channel pulse-height analyzer.

The laser control circuit was unable to prevent slow variations in the laser average intensity due to acoustic vibrations of the movable mirror in the laser resonant cavity. A window discriminator gating unit was constructed that sensed the laser average intensity and gated on the pulse-height analyzer only when the laser average intensity was within $\pm 3\%$ of a preset value. This permitted measurements of $\langle :\hat{I}(\mathbf{x}_1,t_1)\hat{I}(\mathbf{x}_1\, t_1+\tau):\rangle$ as a function of average laser intensity to be made in the threshold region of oscillation. The integrator preceding the input to the window discriminator had a time constant of 20 msec, so that only the slow variations in intensity due to acoustic vibration, and not the fast intensity fluctuations intrinsic to a laser operated near its threshold of oscillation, acted on the window discriminator.

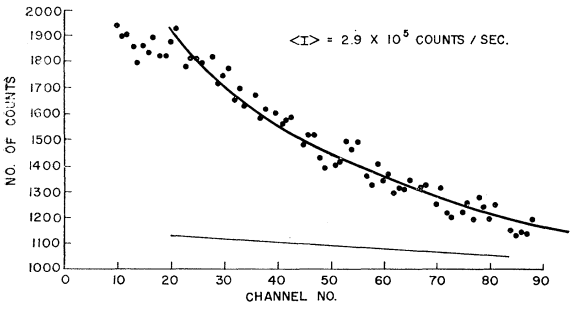

FIG. 3. Plot of the number of counts in each channel of the pulse-height analyzer as a function of channel number.

The window discriminator gating unit was also used to gate a timing arrangement that recorded the length of time that the pulse-height analyzer was allowed to accumulate data, and also could be used to monitor the average photomultiplier tube counting rates. The timing circuit consisted of a stable 100 kc/sec pulse generator, fast discriminators, and fast scalers.

The apparatus used to make measurements of third-order intensity correlation functions is substantially the same, and a block diagram of it is shown in Fig. 2. It differs from that of Fig. 1 in that the output from a coincidence logic unit is used to start the TAC.

The response of the apparatus shown in Figs. 1 and 2 to a source with no observable correlated intensity fluctuations was measured. The photodetectors viewed an incandescent lamp (it had a correlation time of 10^{-13} sec) driven by a stable dc current, instead of the laser source. At the same time, the laser was operated near threshold and the window discriminator gating unit used to gate the pulse-height analyzer and timing circuits was driven by the output of the laser. The response of the apparatus was observed to be that predicted by Eqs. (3c) and (5c). $\xi(\tau)$ and $\xi(\tau_1,\tau_2)$ were observed to be 0.00 ± 0.02 for all values of τ and τ_1,τ_2 measured.

IV. EXPERIMENTAL RESULTS

A. Second-Order Intensity Correlation Functions

A relatively small digital computer (IBM 1130) was used to solve Eq. (3a) for the second-order intensity fluctuation correlation function. The computer first calculated 60 values of $\xi(\tau)$ from data points taken from a smooth curve drawn through the raw data accumulated in the pulse-height analyzer (see Fig. 3).[23] Since some of the integrals in Eq. (3) required values of the integrand not directly measurable, an approximation was made.

The normalized measured excess $\xi(\tau)$ was linearly extrapolated for an additional 30 increments of τ, and

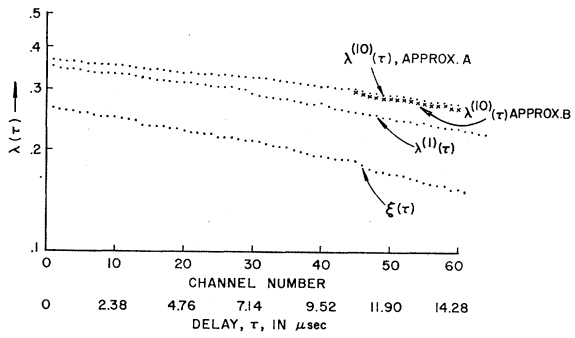

FIG. 4. Plot of the computed solutions to the integral equation for $\lambda(\tau)$ as a function of τ.

[23] Figure 3 is a plot of the number of counts in each channel of the pulse-height analyzer as a function of channel number. The lower solid curve represents the number in each channel expected from a source with no correlated intensity fluctuations.

then set to equal either zero or its last computed value. These values of $\xi(\tau)$ were then used to calculate the first-order solution $\lambda^{(1)}(\tau)$ to the integral Eq. (3a). $\lambda^{(1)}(\tau)$ was used to compute the second-order solution to $\lambda(\tau)$, and so on until the successive computed solutions to $\lambda(\tau)$ differed by less than 0.0001. Fewer than 10 iterations were needed to achieve this. The functions $\lambda(\tau)$ were approximated by $\lambda(90)$ or by 0 for arguments in excess of the first 90 values considered. Figure 4 illustrates the rapid convergence of the iterated solutions for $\lambda(\tau)$ and the negligible difference between the two approximations used in solving the integral equation. Approximation A, which treats $\lambda^{(n)}(\tau)$ as a constant after the first 90 values, clearly overestimates the true solution, and approximation B, which sets $\lambda^{(n)}(\tau)=0$ after the first 90 values, underestimates the final result. In any case, the difference between the two procedures is negligible. The example illustrated is for the worst possible case where $\lambda(\tau)$ remains appreciable over the entire range of values considered. The final solution was considered accurate only for the first 60 values of the computed function.

Measurements to determine $\lambda(\tau)$ were made for 18 different laser average intensities about, and including, the threshold of oscillation. Figure 5 is a plot of the value of $\lambda(\tau)$ at $\tau=0$, $\lambda(0)$, as a function of laser average intensity. Well below threshold, the laser behaves as a thermal source, with $\lambda(0)\approx 1.0$. As threshold is approached and exceeded, $\lambda(0)$ decreases and reaches 0.0 well above the threshold. $\lambda(0)$ is also the counting excess and has been measured by Arecchi *et al.*,[24] Chang *et al.*,[25] Armstrong and Smith,[14] and Freed and Haus.[17] The solid curve is the theoretically expected behavior of $\lambda(0)$ as calculated by Lax and co-workers[26–28] and by other authors as well.[29–34] The mean laser intensity is expressed in terms of the counting rate which the photomultiplier P2 would have shown had there been no attenuating neutral density filters between it and the source. Comparison of experimental and theoretical results was made with the use of one scaling parameter that matched the dimensionless mean intensity of the theoretical laser to the mean intensity of the laser studied at one point, near $\lambda(0)=0.5$. The errors in the experimental values $\lambda(0)$ are estimated as ± 0.02 and result from the statistical uncertainty of the best smooth curve to draw through the raw data points stored on the pulse-height analyzer. These results are in agreement with other experimental determinations of $\lambda(0)$ from photoelectric counting distribution measurements.[14,24,25]

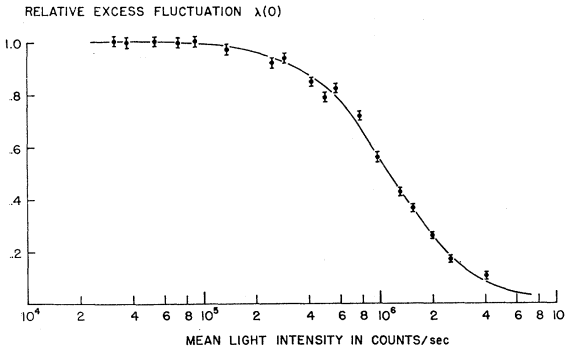

FIG. 5. Plot of the values of $\lambda(\tau)$ at $\tau=0$ as a function of average laser intensity.

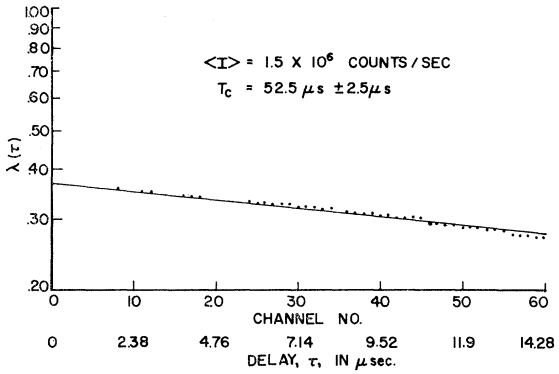

FIG. 6. Plot of the computed values of $\lambda(\tau)$ as a function of τ on a logarithmic scale.

All of the experimentally observed correlation functions $\lambda(\tau)$ were observed to be roughly of the form $\lambda(\tau)=\lambda(0)\exp(-|\tau|/T_c)$ as shown by the example in Fig. 6. Figure 7 is a plot of the decay constants T_c as a function of mean laser intensity. The solid curve is the theoretically expected behavior of the T_c as a function of

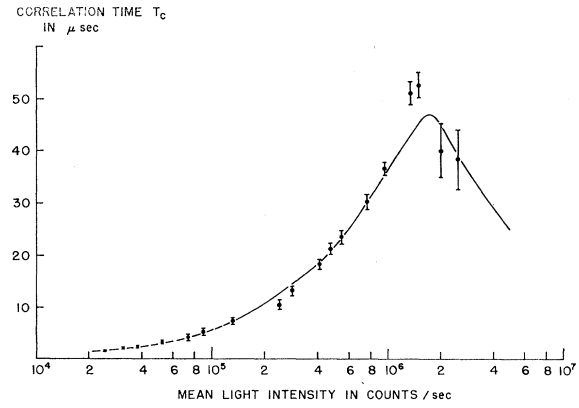

FIG. 7. Plot of the values of the decay constant T_c as a function of average laser intensity on a logarithmic scale.

[24] F. T. Arecchi, G. S. Rodari, and A. Sona, Phys. Letters **25A**, 59 (1967).
[25] R. F. Chang, R. W. Detenbeck, V. Korenman, C. O. Alley, and V. Hochuli, Phys. Letters **25A**, 272 (1967).
[26] M. Lax and W. Louisell, J. Quant. Electron. **QE–3**, 47 (1967).
[27] M. Lax, J. Quant. Electron. **QE–3**, 37 (1967).
[28] R. Hempstead and M. Lax, Phys. Rev. **161**, 350 (1967).
[29] H. Risken, Z. Physik **186**, 85 (1965).
[30] H. Risken, Z. Physik **191**, 302 (1966).
[31] V. Arzt, H. Haken, H. Risken, H. Sauerman, C. Schmid, and W. Weidlich, Z. Physik **197**, 207 (1966).
[32] H. Risken and D. Vollmer, Z. Physik **210**, 323 (1967).
[33] W. Weidlich, H. Risken, and H. Haken, Z. Physik **201**, 396 (1967).
[34] W. Lamb and M. Scully, Phys. Rev. **159**, 208 (1967).

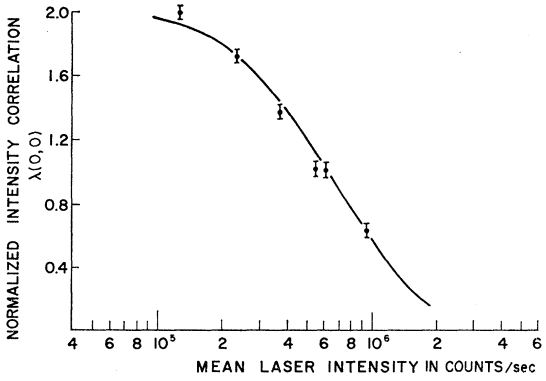

FIG. 8. Plot of the values of $\lambda(0,0)$ as a function of mean laser intensity.

mean laser intensity.[26–33]. Comparison of experimental and theoretical values of T_c was made with the use of the same mean intensity scale factor as in Fig. 4 and one additional scaling parameter that matched the theoretical dimensionless decay constants to the experimentally observed values at one point near $T_c = 20\,\mu$sec. The experimental results are in agreement with those obtained from a spectrum analysis of fluctuations in the output current of a photomultiplier.[17]

The errors in T_c, the value of the decay constant, were obtained by variation of the slopes of the best straight line that could reasonably be drawn through the computed values of $\lambda(\tau)$ plotted on semilogarithmic graph paper as a function of τ. They were found to be $\pm 5\%$ for mean intensities below the peak in Fig. 5. Because of the low values of $\lambda(\tau)$ and fixed uncertainty of ± 0.02 in them, the errors in T_c were $\pm 10\%$ for mean intensities above the peak in Fig. 5.

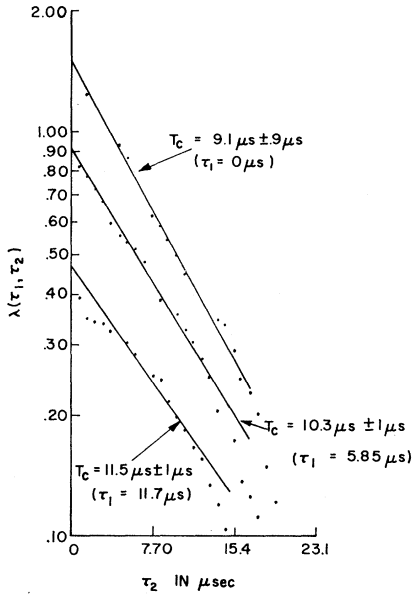

FIG. 9. Plot of the values of $\lambda(\tau_1,\tau_2)$ as a function of τ_2 for a fixed value of τ_1 on a logarithmic scale.

TABLE I. Experimental results for second- and third-order intensity correlation function decay constants.

Mean light intensity (10^5 counts/sec)	Time constant for decay of $\lambda(\tau)$ with τ in μ sec	Time constant for decay of $\lambda(\tau_1,\tau_2)$ with τ_1 in μ sec ($\tau_2=0$)	Time constant for decay of λ (τ_1,τ_2) with τ_2 in μ sec
			6.4±0.6($\tau_1=0$)
1.3	6.2±0.6	6.4±0.6	6.6±0.6($\tau_1=2.73\,\mu$sec)
			7.3±0.6($\tau_1=5.85\,\mu$sec)
			9.1±1.0($\tau_1=0$)
2.4	10.7±1.2	9.5±1.0	10.3±1.0($\tau_1=5.85\,\mu$sec)
			11.5±1.0($\tau_1=11.7\,\mu$sec)
			16 ±1.6($\tau_1=0$)
5.6	27.6±0.2	18 ±1.5	14.2±1.4($\tau_1=8.55\,\mu$sec)
			17 ±2 ($\tau_1=0$)
9.6	36 ±1.8	16 ±2	19 ±2 ($\tau_1=8.55\,\mu$sec)

B. Third-Order Intensity Correlation Functions

A digital computer was used to solve Eq. (6) for the desired intensity correlation function $\lambda(\tau_1,\tau_2)$ by iteration. The zeroth-order solution to Eq. (6) was computed from $\xi(\tau_1,\tau_2)$ and measurements made to determine $\lambda(\tau)$ immediately preceding those made to determine $\lambda(\tau_1,\tau_2)$. The values of τ_1 used were not large enough to require extrapolation procedures to determine measured values of the integrands in Eq. (6). The computed solutions $\lambda^{(n)}(\tau_1,\tau_2)$ again converged rapidly (less than 10 iterations).

Measurements were made to determine $\lambda(\tau_1,\tau_2)$ as a function of τ_1 and τ_2 at several laser average intensities in the threshold region. Figure 8 is a plot of $\lambda(0,0)$ as a function of mean laser intensity. $\lambda(0,0)$ is closely related to the third moment of counting distribution, and has been measured by Chang *et al.*[25] The solid curve is the theoretically expected behavior of $\lambda(0,0)$ in the threshold region as computed from the work in Ref. 28. The errors in $\lambda(0,0)$ are estimated at ± 0.06 and result from the dependence of $\lambda(\tau_1,\tau_2)$ on three

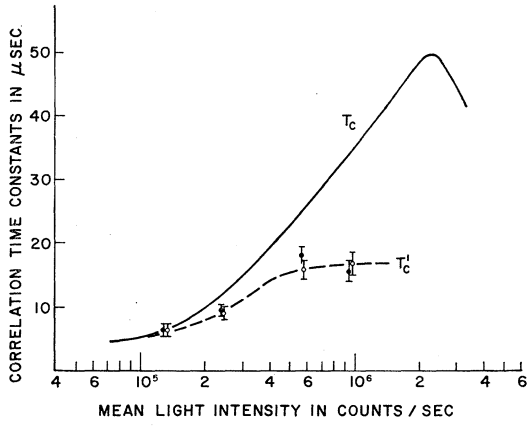

FIG. 10. Plot of the values of T_c' as a function of mean laser intensity.

experimentally determined functions of the type $\lambda(\tau)$, each of which can be determined to an accuracy of ± 0.02.

All of the experimentally observed correlation functions $\lambda(\tau_1,\tau_2)$ were observed to be approximately of the form $\lambda(\tau_1,\tau_2)=\lambda(0,0)\exp(-|\tau_1|/T_c')\exp(-|\tau_2|/T_c')$ as shown by the example in Fig. 9. Well below threshold T_c' was observed to be equal to T_c, the second-order intensity fluctuation correlation decay constant. As the threshold of oscillation was approached, T_c' was observed to depart increasingly from T_c. [Table I lists the decay constants T_c and T_c' of the correlation function $\lambda(\tau)$ and $\lambda(\tau_1,\tau_2)$ with respect to τ, τ_1, and τ_2.]

Figure 10 is a plot of T_c' as a function of mean laser intensity. The solid curve represents the behavior of T_c in the threshold region. The values of T_c that resulted from measurements made to determine the function $\lambda(\tau)$ to be used in calculating $\lambda(\tau_1,\tau_2)$ from Eq. (6) were in agreement with the solid curve. No theoretical decay constants T_c' for the third-order intensity fluctuation correlation functions as a function of mean laser intensity in the threshold region have been calculated so far.

PHYSICAL REVIEW VOLUME 185, NUMBER 2 10 SEPTEMBER 1969

Dielectric Relaxation in Alkaline-Earth Fluoride Crystals*

J. H. CHEN AND M. S. MCDONOUGH†‡
Physics Department, Boston College, Chestnut Hill, Massachusetts 02167
(Received 12 March 1969)

Dielectric absorption has been investigated over a temperature range from −34 to 450°C and a frequency range from 1 to 10^5 cps for doped CaF_2, BaF_2, and SrF_2 crystals. The activation and association energies for the dipolar complexes have been determined. The activation energy for CaF_2 doped with 0.01-mole% YF_3 was found to be 1.17 eV.

I. INTRODUCTION

THE effects produced by the doping of ionic crystals with known concentrations of aliovalent cations can be investigated using various techniques. Several investigations have shown that the predominant intrinsic defects in CaF_2-type crystals are Frenkel anion pairs.[1–3] When a trivalent ion replaces a positive divalent ion in the lattice of an alkaline-earth fluoride crystal, a singly charged negative ion interstitial may be introduced into a next-nearest-neighbor position as a charge compensator. A dipolar complex results from the cation impurity possessing an extra positive charge, and the interstitial possessing an effective negative charge.

Both Zintl and Udgard[1] and Short and Roy[2] have shown that a dissolved trivalent yttrium ion is accompanied by an interstitial fluorine ion. With the aid of conductivity experiments, Ure[3] has shown that a trivalent yttrium ion is associated with an interstitial fluorine ion, and a sodium ion is associated with a fluorine vacancy. Also, electron paramagnetic studies of rare-earth-doped alkaline-earth fluoride crystals have demonstrated that the rare-earth site has tetragonal symmetry which may be explained by the presence of a charge compensating fluorine interstitial at a nearest-neighbor position.[4]

Dielectric measurements on the alkaline-earth fluorides have been previously reported.[5–7] Our investigations have been principally concerned with dielectric relaxation in doped CaF_2, BaF_2, and SrF_2.[8] The phenomena observed can be described in terms of the relaxation mechanisms originated by Debye[9] and later applied to crystal imperfections by Breckenridge.[10] Using the method described by Lidiard[11] the expression for an alkaline-earth fluoride crystal of the loss tangent, for a single loss mechanism possessing a unique relaxation time is

$$\tan\delta=(4\pi a^2e^2N_ip/3kT\epsilon)\omega\tau/(1+\omega^2\tau^2),$$

where a is the anion-cation separation, e is the electronic charge, N_i is the concentration of the impurity ion, p is the degree of association, k is Boltzmann's constant, T is the absolute temperature, ϵ is the static dielectric constant of the crystal, ω is the angular frequency of the applied electric field, and τ is the relaxation time. The

* Work supported in part by the National Science Foundation.
† Present address: Panametrics, Inc., Waltham, Mass.
‡ Based in part on work submitted by M.S.M. as a thesis in partial fulfillment of the requirements for the doctoral degree at Boston College.
[1] E. Zintl and A. Udgard, Z. Anorg. Allgem. Chem. **240**, 150 (1939).
[2] J. Short and R. Roy, J. Phys. Chem. **67**, 1860 (1963).
[3] R. W. Ure, Jr., J. Chem. Phys. **26**, 1441 (1957).
[4] B. Bleaney, P. M. Llewellyn, and D. A. Jones, Proc. Phys. Soc. (London) **69I3**, 858 (1956).
[5] G. Jacobs, J. Chem. Phys. **27**, 1441 (1957).
[6] T. E. Nikitinskaya and T. V. Bol'shakova, Fiz. Tverd. Tela **3**, 3224 (1961) [English transl.: Soviet Phys.—Solid State **3**, 2340 (1961)].
[7] P. D. Southgate, Bull. Am. Phys. Soc. **11**, 195 (1966).
[8] J. H. Chen and M. S. McDonough, Bull. Am. Phys. Soc. **9**, 647 (1964).
[9] P. Debye, *Polar Molecules* (The Chemical Catalog Company, Inc., 1929).
[10] R. G. Breckenridge, J. Chem. Phys. **16**, 959 (1948).
[11] A. B. Lidiard, in *Handbuch Der Physik*, edited by S. Flügge (Springer-Verlag, Berlin, 1957), Vol. XX.